A Simple and Robust Digital Current Control for a PM Synchronous Motor under the Parameter Variations

Kyeong-Hwa Kim, In-Cheol Baik, and Myung-Joong Youn

Abstract

A simple and robust digital current control technique for a permanent magnet (PM) synchronous motor under the parameter variations is presented. Among the various current control schemes for an inverter-fed PM synchronous motor drive, the predictive control is known to give a superior performance. This scheme, however, requires the full knowledge of machine parameters and operating conditions, and cannot give a satisfactory response under the parameter mismatch. To overcome such a limitation, the disturbances caused by the parameter variations will be estimated by using a disturbance observer theory and used for the computation of the reference voltages by a feedforward control. Thus, the steady-state control performance can be significantly improved with a relatively simple control algorithm, while retaining the good characteristics of the predictive control. The proposed control scheme is implemented on a PM synchronous motor using the software of DSP TMS320C30 and the effectiveness is verified through the comparative simulations and experiments.

I. Introduction

PM synchronous motors have been gradually replacing DC motors in a wide range of drive applications such as machine tools and industrial robots. The advantage of using a PM synchronous motor is that many drawbacks caused by the brushes and commutators of a DC motor can be eliminated. Furthermore, the PM synchronous motor has the high power density, large torque to inertia ratio, and high efficiency as compared with a DC motor having the same output rating [1], [2]. The PM synchronous motor, however, has the nonlinear characteristics and inherent coupling problem. Therefore, to directly control the developed torque, the field-oriented control is usually employed. In the high performance field-oriented control system, the torque and flux producing components of the stator current are decoupled so that the independent torque and flux controls are possible as in DC motors. Thus, a high quality current control is essential for the successful implementation of the field-oriented control since the current controller has a direct influence on the drive performance [3], [4].

Manuscript received December 26, 1997; accepted January 21, 1998.

K. H Kim, I. C. Baik and M. J. Youn are with the Department of Electrical Engineering Korea Advanced Institute of Science and Technology.

The current control schemes for an inverter-fed PM synchronous motor drive can be classified as the hysteresis control, ramp comparison control, synchronous frame proportional-integral (PI) control, and predictive control [4]-[11]. The basic requirements for the current controller are the fast dynamic response during the transient state, lower current ripple in the steady-state, stable PWM inverter operation, and robustness against the variations of machine parameters. The hysteresis current control has the advantages such as a fast transient response and a simple implementation. However, because of large current errors and an irregular PWM inverter operation, this scheme cannot be used in a high performance drive system [4]. The ramp comparison current control scheme gives a constant switching frequency. However, there are some unavoidable limitations such as a steady-state error and a phase delay in the steady-state since this controller is designed in the stationary reference frame where P or PI controller can not exactly track the sinusoidally varying reference [4]. To overcome such a limitation, a synchronous frame PI current regulator has been proposed [5]. In the synchronous frame PI current regulator, the regulated currents are dc quantities rather than the variables as in the stationary reference frame. By employing the PI control and cancellation inputs for the back EMF and cross-coupling terms, this control gives an ideal steady-state control characteristics irrespective of operating conditions.

However, the transient response is generally slow or may be degraded due to the inexact cancellation input under the parameter variations. On the other hand, in a predictive control scheme, the switching instants of the inverter switches are determined by calculating the required voltage which forces the motor currents to follow their references. With the space vector PWM technique, this control scheme is known to provide the advantages such as a constant switching frequency and a lower current ripple [6], [7]. This scheme, however, requires the full knowledge of machine parameters and operating conditions with the sufficient accuracy, and cannot give a satisfactory response under the parameter mismatch. Generally, it is very difficult to exactly obtain the informations on the machine parameters since they may vary during operation due to the changes in the temperature, current level, and operating frequency. In particular, the inaccuracy of the back EMF influences primarily on the control performance. To overcome such a problem, a current control scheme independent of the back EMF variation has been proposed [8], [9]. The basic assumption is that the back EMF is constant between each sampling instant. Based on this, the back EMF has been estimated by using the feedback of the delayed input voltages and currents in a discrete domain. Thus, a robust control performance against the back EMF variation can be obtained. This scheme still, however, requires other motor parameters such as the stator resistance and stator inductance, and also unstable regions may exist under a certain variation of the stator inductance. Recently, a multivariable state feedback control with an integrator [10] and a generalized predictive control [11] have been reported. Although a good performance can be obtained, the controller design is quite complex. In view of the robustness against a certain disturbance, it is well known that the use of a disturbance observer is very effective. Though the disturbance is not a state, the conventional observer can be easily extended under the assumption that an unknown disturbance is a constant during each sampling interval [12]-[15].

This paper presents a simple and robust digital current control technique for a PM synchronous motor under the parameter variations. Although the predictive control provides an ideal response and a stable performance independent of the operating condition, its steady-state response may be degraded under the motor parameter variations such as the flux linkage, stator inductance, and stator resistance. This is more serious at high speed operations since the disturbance is proportional to the product of the operating speed and these parameters.

To overcome this drawback, the disturbance voltages caused by the parameter variations will be estimated by using a disturbance observer and used for the calculation of the reference voltages by a feedforward control. Thus, the steady-state control performance can be significantly improved, while retaining the good characteristics of the predictive control. Since the reduced-order observer is used for the disturbance estimation, the observer design is considerably simple. As a result, an improved robustness against the parameter variations can be obtained without requiring a much more complex controller design such as the methods in [8], [10]. The whole control processing is implemented by the software of DSP TMS320C30 for a PM synchronous motor driven by a three-phase voltage-fed PWM inverter.

II. Modeling of PM Synchronous Motor

A PM synchronous motor considered in this paper consists of permanent magnets mounted on the rotor surface and three phase stator windings which are sinusoidally distributed and displaced by 120° . The stator voltage equations of a PM synchronous motor in the synchronous reference frame are described as follows [1]:

$$v_{qs} = R_s i_{qs} + L_s \dot{i}_{qs} + L_s \omega_r i_{ds} + \lambda_m \omega_r \tag{1}$$

$$v_{ds} = R_s i_{ds} + L_s \dot{i}_{ds} - L_s \omega_r i_{qs} \tag{2}$$

where R_s is the stator resistance, L_s is the stator inductance, ω_r is the electrical rotor angular velocity, and λ_m is the flux linkage established by the permanent magnet. From (1) and (2), the discrete-time equation can be obtained as follows:

$$v_{qs}(k) = R_s i_{qs}(k) + \frac{L_s}{T}[i_{qs}(k+1) - i_{qs}(k)] + L_s \omega_r i_{ds}(k) + \lambda_m \omega_r \tag{3}$$

$$v_{ds}(k) = R_s i_{ds}(k) + \frac{L_s}{T}[i_{ds}(k+1) - i_{ds}(k)] - L_s \omega_r i_{qs}(k) \tag{4}$$

where T is a sampling period. Using the nominal parameters, (3) and (4) can be rewritten as follows:

$$\begin{aligned} v_{qs}(k) = {} & R_{so} i_{qs}(k) + \frac{L_{so}}{T}[i_{qs}(k+1) - i_{qs}(k)] \\ & + L_{so} \omega_r i_{ds}(k) + \lambda_{mo} \omega_r + f_q(k) \end{aligned} \tag{5}$$

$$v_{ds}(k) = R_{so} i_{ds}(k) + \frac{L_{so}}{T}[i_{ds}(k+1) - i_{ds}(k)] - L_{so} \omega_r i_{qs(k)} + f_{d(k)} \tag{6}$$

where $f_q(k)$ and $f_d(k)$ represent the disturbances caused by the parameter variations. These can be expressed as

$$\begin{aligned} f_q(k) = {} & \Delta R_s i_{qs}(k) + \frac{\Delta L_s}{T}[i_{qs}(k+1) - i_{qs}(k)] \\ & + \Delta L_s \omega_r i_{ds}(k) + \Delta \lambda_m \omega_r \end{aligned} \tag{7}$$

$$f_d(k) = \Delta R_s i_{ds}(k) + \frac{\Delta L_s}{T}[i_{ds}(k+1) - i_{ds}(k)] - \Delta L_s \omega_r i_{qs}(k) \tag{8}$$

where $\Delta R_s = R_s - R_{so}$, $\Delta L_s = L_s - L_{so}$, $\Delta \lambda_m = \lambda_m - \lambda_{mo}$ and subscript "o" denotes the nominal value. Using $i_{qs}(k)$ and $i_{ds}(k)$ as the state variables, the discrete-time state equation of a PM synchronous motor can be expressed as follows:

$$\begin{pmatrix} i_{qs}(k+1) \\ i_{ds}(k+1) \end{pmatrix} = \begin{pmatrix} 1-\frac{R_{so}}{L_{so}}T & -\omega_r T \\ \omega_r T & 1-\frac{R_{so}}{L_{so}}T \end{pmatrix} \begin{pmatrix} i_{qs}(k) \\ i_{ds}(k) \end{pmatrix} + \frac{T}{L_{so}} \begin{pmatrix} v_{qs}(k) \\ v_{ds}(k) \end{pmatrix} - \frac{T}{L_{so}} \begin{pmatrix} f_q(k) \\ f_d(k) \end{pmatrix} + \begin{pmatrix} -\frac{T}{L_{so}}\lambda_{mo}\omega_r \\ 0 \end{pmatrix}. \quad (9)$$

III. System Augmentation and Disturbance Observer

The effective approach to improve the steady-state response with a simple control algorithm is to employ a disturbance observer technique. It is noted that the unknown disturbances $f_q(k)$ and $f_d(k)$ defined in (7) and (8) are not the state variables but the disturbances caused by the parameter variations. The conventional observer can be easily extended to estimate these disturbances. If the observer has a sufficiently fast dynamics as compared with the time variation of these disturbances, it can be assumed that the variations of $f_q(k)$ and $f_d(k)$ are nearly zero during each sampling interval as follows [12]-[15]:

$$f_q(k+1) = f_q(k) \quad (10)$$

$$f_d(k+1) = f_d(k). \quad (11)$$

Under this assumption, $f_q(k)$ and $f_d(k)$ can be regarded as the additional state variables. Then, from the discrete-time state equation in (9), and the additional two state variables in (10) and (11), the augmented state equation is given as follows:

$$\begin{pmatrix} x_a(k+1) \\ x_b(k+1) \end{pmatrix} = \begin{pmatrix} A_{11} & A_{12} \\ A_{21} & A_{22} \end{pmatrix} \cdot \begin{pmatrix} x_a(k) \\ x_b(k) \end{pmatrix} + \begin{pmatrix} B_1 \\ B_2 \end{pmatrix} v_s(k) + \begin{pmatrix} d_1 \\ d_2 \end{pmatrix} = Ax(k) + Bv_s(k) + d \quad (12)$$

$$y(k) = C \begin{pmatrix} x_a(k) \\ x_b(k) \end{pmatrix} \quad (13)$$

where $x_a(k) = [\, i_{qs}(k) \;\; i_{ds}(k)]^T$

$x_b(k) = [\, f_q(k) \;\; f_d(k)]^T$

$v_s(k) = [\, v_{qs}(k) \;\; v_{ds}(k)]^T$

$$A_{11} = \begin{pmatrix} 1-\frac{R_{so}}{L_{so}}T & -\omega_r T \\ \omega_r T & 1-\frac{R_{so}}{L_{so}}T \end{pmatrix}, \; A_{12} = -\frac{T}{L_{so}} \cdot I, \; A_{21} = O, \; A_{22} = I$$

$$B_1 = \frac{T}{L_{so}} \cdot I, \quad B_2 = O$$

$$d_1 = \begin{pmatrix} -\frac{T}{L_{so}}\lambda_{mo}\omega_r \\ 0 \end{pmatrix}, \quad d_2 = \begin{pmatrix} 0 \\ 0 \end{pmatrix}$$

$$C = [\, I \;\; O], \quad I = \begin{pmatrix} 1 & 0 \\ 0 & 1 \end{pmatrix}, \quad O = \begin{pmatrix} 0 & 0 \\ 0 & 0 \end{pmatrix}.$$

The observability matrix of the system in (12) and (13) becomes as follows:

$$W = [\; C^T \;\; A^T C^T \;\; \cdots \;\; (A^T)^{n-1} C^T \;]. \quad (14)$$

Since the rank of a matrix W is 4, the full state vector is completely observable. However, the system states are decomposed of the state variables that can be directly measurable and unmeasurable states. To simply estimate these unmeasurable states, a reduced-order observer can be used as follows:

$$\hat{x}_b(k+1) = (A_{22} - LA_{12})\,\hat{x}_b(k) + A_{21}x_a(k) + B_2 v_s(k) + d_2 + L[x_a(k+1) - A_{11}x_a(k) - B_1 v_s(k) - d_1] \quad (15)$$

where the symbol "^" denotes the estimated quantities and L is an observer gain matrix defined as

$$L = \begin{pmatrix} l_1 & l_2 \\ l_3 & l_4 \end{pmatrix}. \quad (16)$$

Since the measured value of $x_a(k+1)$ is needed to estimate $\hat{x}_b(k+1)$, a new state variable is defined as follows [16]:

$$x_c(k) = \hat{x}_b(k) - Ly(k) = \hat{x}_b(k) - Lx_a(k). \quad (17)$$

In terms of this state $x_c(k)$, the observer for the disturbance estimation is given as follows:

$$x_c(k+1) = (A_{22} - LA_{12})\,\hat{x}_b(k) + d_2 - Ld_1 + (A_{21} - LA_{11})x_a(k) + (B_2 - LB_1)v_s(k) \quad (18)$$

$$\hat{x}_b(k) = x_c(k) + Lx_a(k). \quad (19)$$

Fig. 1 shows the configuration of the reduced-order observer for the disturbance estimation. If the estimation error is chosen as

$$e(k) = x_b(k) - \hat{x}_b(k) \quad (20)$$

then the error dynamics of the observer can be expressed as follows:

$$e(k+1) = (A_{22} - LA_{12}) \cdot e(k). \quad (21)$$

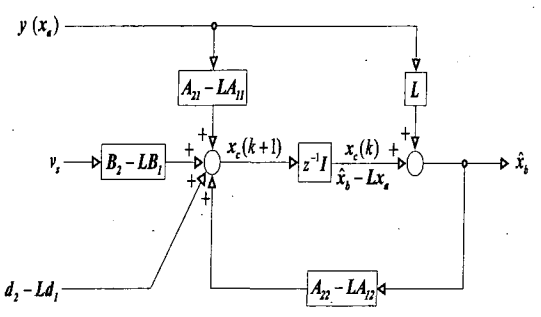

Fig. 1. Reduced-order observer for the disturbance estimation

The dynamic characteristics of the observer can be determined by the eigenvalues of the matrix $(A_{22} - LA_{12})$,

which can be obtained by the characteristics equation as follows:

$$det|zI-(A_{22}-LA_{12})| = z^2-\left(2+\frac{l_1+l_4}{L_{so}}T\right)z. \\ +\left(1+\frac{l_1+l_4}{L_{so}}T+\frac{l_1l_4-l_2l_3}{L_{so}^2}T^2\right)=0 \quad (22)$$

The selection of the observer poles requires a compromise between the rapidity of the response and the sensitivity to the measurement noise. The poles of the observer in the continuous-time domain, $-\alpha\pm j\beta$ can be transferred to the discrete-time domain through the transformation of $z= e^{Ts}$ as follows:

$$\zeta\pm j\eta = e^{-\alpha T}(\cos\beta T\pm j\sin\beta T). \quad (23)$$

Thus, if the observer poles in the continuous-time domain is determined, the pole locations in z-domain, and thus, the observer gains can be easily obtained by the pole placement technique.

IV. Current Control with Simple Feedforward Disturbance Compensation Scheme

In the nominal conditions of $f_q(k)=f_d(k)=0$, the predictive control provides an ideal response irrespective of operating conditions. However, the motor parameters may vary during the operation. Also, the exact modeling is generally very difficult. In these circumstances, $f_q(k)$ and $f_d(k)$ are the functions of the operating speed and current. The influences of such disturbances on the current control performance are more serious at high speed operations under the variations of the flux linkage and stator inductance.

The steady-state control performance of the predictive current control can be significantly improved through the use of a disturbance compensation technique, while retaining its good dynamic performance. By employing the estimated disturbances $\hat{f}_q(k)$ and $\hat{f}_d(k)$ for a feedforward control and replacing $i_{qs}(k+1)$ and $i_{ds}(k+1)$ with their references in (9), the reference voltages in the proposed control scheme are calculated as follows:

$$v_{qs}^*(k)=R_{so}i_{qs}(k)+\frac{L_{so}}{T}[i_{qs}^*(k+1)-i_{qs}(k)] \\ +L_{so}\omega_r(k)i_{ds}(k)+\lambda_{mo}\omega_r(k)+\hat{f}_q(k) \quad (24)$$

$$v_{ds}^*(k)=R_{so}i_{ds}(k)+\frac{L_{so}}{T}[i_{ds}^*(k+1)-i_{ds}(k)] \\ -L_{so}\omega_r(k)i_{qs}(k)+\hat{f}_d(k) \quad (25)$$

where the symbol "*" denotes the reference quantities. Then, the reference voltages are composed of the conventional predictive control part and disturbance compensation part.

The steady-state performance due to the inaccuracy of the machine parameters can be obtained from the reference voltages and the discrete-time voltage equations in (5) and (6). The calculated reference voltages are applied to a PM synchronous motor through the PWM technique. For the simplification of analysis, it is reasonable to assume that the reference voltages are applied to the terminals of the motor without any loss and deformation in the PWM inverter, i.e., $v_{qs}^*(k)=v_{qs}$ and $v_{ds}^*(k)=v_{ds}$. Under this assumption, the steady-state current errors can be analytically obtained. When the conventional predictive control is used without a feedforward compensation of $\hat{f}_q(k)$ and $\hat{f}_d(k)$, the q-axis and d-axis current errors at the $(k+1)$-th sampling instant can be derived from the reference voltages and the discrete-time voltage equations as follows:

$$i_{qs}^*(k+1)-i_{qs}(k+1)=\frac{T}{L_{so}}f_q(k) \quad (26)$$

$$i_{ds}^*(k+1)-i_{ds}(k+1)=\frac{T}{L_{so}}f_d(k). \quad (27)$$

Clearly, the steady-state errors are proportional to the magnitude of disturbances which is the function of an operating speed and a load condition. The steady-state q-axis and d-axis current errors of the predictive control at the $(k+1)$-th sampling instant due to the inaccuracy of the individual machine parameters are summarized in Table I. On the contrary, the steady-state current errors of the proposed control scheme at the $(k+1)$-th sampling instant can be obtained from the reference voltages and the discrete-time voltage equations as follows:

$$i_{qs}^*(k+1)-i_{qs}(k+1)=\frac{T}{L_{so}}e_q(k) \quad (28)$$

$$i_{ds}^*(k+1)-i_{ds}(k+1)=\frac{T}{L_{so}}e_d(k) \quad (29)$$

where $e(k)=[e_q(k)\ \ e_d(k)]^T$. Unlike the conventional predictive control, where the steady-state current errors are dependent on the magnitude of the disturbances, the current errors of the proposed control scheme are proportional to the estimation error of the disturbances. Thus, as the estimated disturbances converge to their real values, the steady-state current errors will be removed.

Table 1. Steady-state current errors of the predictive control due to the inaccuracy of the individual machine parameters

	$i_{qs}^*(k+1)-i_{qs}(k+1)$	$i_{ds}^*(k+1)-i_{ds}(k+1)$
ΔR_s	$\Delta R_s\left(\frac{T}{L_{so}}\right)i_{qs}(k)$	$\Delta R_s\left(\frac{T}{L_{so}}\right)i_{ds}(k)$
ΔL_s	$\left(\frac{\Delta L_s}{L_{so}}\right)[i_{qs}(k+1)-i_{qs}(k)]$ $+\Delta L_s\left(\frac{T}{L_{so}}\right)\omega_r(k)i_{ds}(k)$	$\left(\frac{\Delta L_s}{L_{so}}\right)[i_{ds}(k+1)-i_{ds}(k)]$ $-\Delta L_s\left(\frac{T}{L_{so}}\right)\omega_r(k)i_{qs}(k)$
$\Delta\lambda_m$	$\Delta\lambda_m\left(\frac{T}{L_{so}}\right)\omega_r(k)$	0

V. Configurations of the Overall Systems

The overall block diagram for the proposed control scheme is shown in Fig. 2. The overall system consists of a proposed current controller, a disturbance observer, a PWM inverter, and a PM synchronous motor. In this figure, the shaded area represents the observer for the disturbance voltage estimation. For the current control algorithm, the predictive control with a feedforward disturbance compensation is used. By using this technique, the reference voltages are composed of the predictive control part and disturbance compensation part. During the operations, the disturbances caused by the parameter variations are estimated by using a reduced-order disturbance observer and used for the feedforward control.

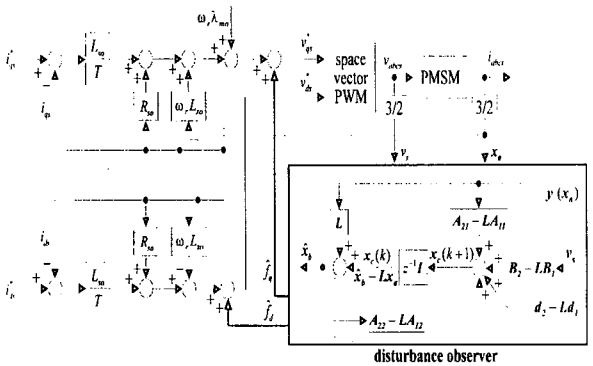

Fig. 2. Overall block diagram for the proposed current control scheme

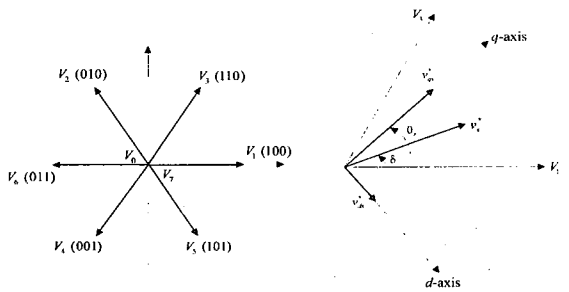

(a) inverter voltage space vectors (b) vector diagram for the computation example

Fig. 3. Computation of the conduction periods

The computed reference voltage vector $v_s^*(k)$ is applied to a PM synchronous motor using the space vector PWM technique [17]. Based on this technique, the conduction periods of the inverter switches are modulated according to the amplitude and angle of the reference voltage vector to obtain the average voltage equal to the reference. Fig. 3(a) shows the voltage space vectors and the corresponding switching states in a three-phase PWM inverter. Fig. 3(b) shows the computation example of the space vector PWM technique. In this figure, the time durations of V_1, V_3, and the zero voltage vector are given by

$$t_A=\sqrt{3}\frac{|v_s^*|}{V_{DC}}\sin(60^\circ-\delta)\cdot T \tag{30}$$

$$t_B=\sqrt{3}\frac{|v_s^*|}{V_{DC}}\sin\delta\cdot T \tag{31}$$

$$t_Z=T-(t_A+t_B) \tag{32}$$

where V_{DC} is a dc link voltage. Also $|v_s^*|$ and δ are given as

$$|v_s^*|=\sqrt{v_{qs}^{*2}+v_{ds}^{*2}}$$

$$\delta=\theta_r-\tan^{-1}\left(\frac{v_{ds}^*}{v_{qs}^*}\right)$$

where θ_r is the electrical rotor angular position. It has been shown that during the large transient periods such as a starting and a sudden load change, the average voltage equal to v_s^* cannot be produced since v_s^* is too large to be synthesized in one switching period. To approximate the average voltage to the reference under such a condition, the time durations of the inverter switches are simply adjusted as follows [18]:

$$t_A'=\frac{t_A}{t_A+t_B}\cdot T \tag{33}$$

$$t_B'=\frac{t_B}{t_A+t_B}\cdot T \tag{34}$$

$$t_Z'=0. \tag{35}$$

Based on this, the feedback voltage for the observer can be easily obtained from the switching states of the inverter and dc link voltage by considering the dead time of the switch.

The configuration of the experimental system is shown in Fig. 4. The whole control algorithms are implemented by the assembly language program using DSP TMS320C30 with a clock frequency of 32 MHz [19], [20]. The sampling period is set to 128 [μsec] both in the simulations and experiments, which yields a switching frequency of 7.8 kHz. The PM synchronous motor is driven by a three-phase PWM inverter employing the intelligent power module (IPM). The rotor speed and absolute rotor position are detected through a 12 bit/rev resolver-to-digital converter (RDC) using a brushless resolver. The phase currents are detected by the Hall-effect devices and are converted through two 12 bit A/D converters, where the resolution of current is $8/2^{11}$ [A]. The detected phase currents are transformed to dq values in a DSP using the rotor position. The nominal parameters of a PM synchronous motor are listed in Table II.

Table 2. Specifications of a PM synchronous motor

Rated power	400 W	Rated speed	3000 rpm
Rated torque	1.274 Nm	Number of poles	4
Magnetic flux	0.16 Wb	Stator resistance	3.0 Ω
Stator inductance	5 mH	Moment of inertia	1.54×10^{-4}Nm $\times\cdot S^2$

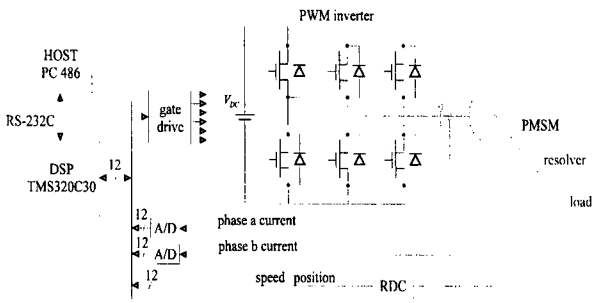

Fig. 4. Configuration of experimental system

VI. Simulations and Experimental Results

In this section, the simulations and experimental results are presented to verify the feasibility of the proposed control scheme under the various conditions. For the performance comparisons with the proposed control scheme, the predictive current control is employed.

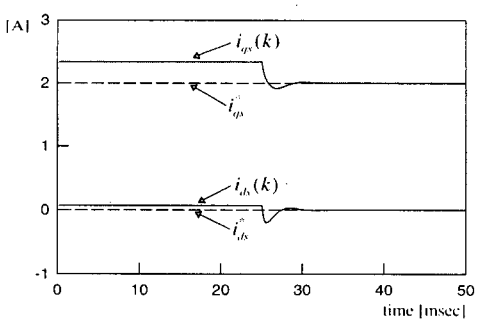

(a) q-axis and d-axis current responses

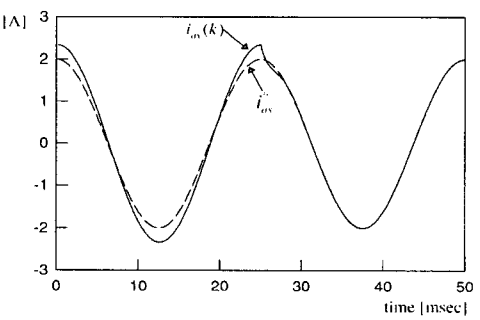

(b) a-phase current at sampling instant

Fig. 5. Control performance of the proposed current control scheme at steady-state under the parameter variations ($\Delta\lambda_m=-0.5\lambda_{mo}$, $\Delta L_s=1.0L_{so}$, and $\Delta R_s=1.0R_{so}$)

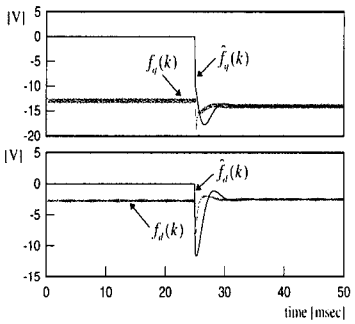

(c) estimated disturbances

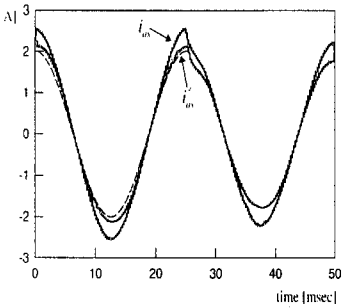

(d) a-phase current response

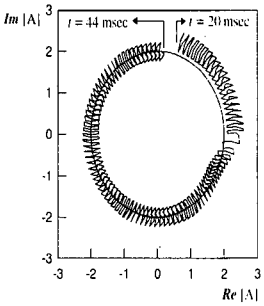

(e) current trajectory

Fig. 5. (Continued)

Fig. 5 shows the simulation results for the proposed control scheme at steady-state under the parameter variations ($\Delta\lambda_m=-0.5\lambda_{mo}$, $\Delta L_s=1.0L_{so}$, and $\Delta R_s=1.0R_{so}$). The q-axis and d-axis current references are given as 2 [A] and zero, respectively, and the motor is operated at a constant speed of 1200 [rpm]. Fig. 5(a) shows the q-axis and d-axis current responses. Fig. 5(b) shows the a-phase current at each sampling instant. Even though the predictive control gives an ideal characteristics for the nominal parameter values ($f_q(k)=f_d(k)=0$), the steady-state errors are observed in the q-axis and d-axis current responses under the parameter mismatch. Also, it can be shown that a phase delay exists in the phase current response. This degradation is expected to be more severe at high speed operations because the magnitude of the disturbances is proportional to an operating speed.

However, as soon as the estimation algorithm starts at 25 [msec] and the estimated disturbances are used for a feedforward control, the steady-state current error and phase delay are quickly removed within 5 [msec]. This can be explained by the estimation of the disturbance voltages as shown in Fig. 5(c). For the design of the observer gain L, $\alpha=\beta=800$ is chosen. The corresponding z-domain observer poles are determined using (23) as $\zeta\pm j\eta=0.898\pm j0.0923$. Thus, using (22) and the pole placement technique, L can be

obtained as follows:

$$L=\begin{pmatrix} -3.984 & -3.601 \\ 3.601 & -3.984 \end{pmatrix}.$$

The corresponding a-phase current response is shown in Fig. 5(d). Also the current trajectory in the complex plane is shown in Fig. 5(e). It can be clearly shown that the influence of the disturbances due to the parameter variations can be effectively suppressed by using the proposed control scheme.

Fig. 6 shows the experimental results for the proposed current control scheme under $\Delta\lambda_m=-0.5\lambda_{mo}$. Similarly, the q-axis and d-axis current references are given as 2 [A] and zero, respectively. Also, the observer gains are selected as the same as the simulation conditions. Before the estimation algorithm starts, a steady-state error of 0.7 [A] is observed in the q-axis current response. However, this steady-state error is removed within 4 [msec] as soon as the estimation algorithm starts and the estimated values are used for the feedforward control. The corresponding a-phase current and the estimating performance of the observer are shown in Fig. 6(b).

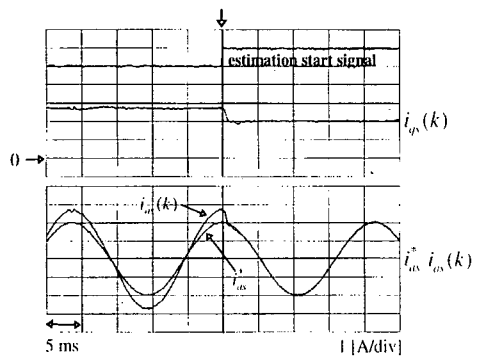

(a) q-axis current and a-phase current at sampling instant

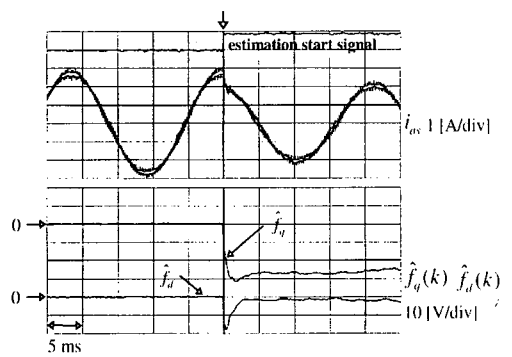

(b) a-phase current and estimated disturbances

Fig. 6. Control performance of the proposed current control scheme at steady-state under $\Delta\lambda_m=-0.5\lambda_{mo}$

Figs. 7 and 8 show the current responses under $\Delta L_s=0.8L_{so}$. In the conventional predictive control, the phase delay between the reference and measured value is clearly present as can be seen in Fig. 7. Also, some d-axis current exists (0.5 [A]), which degrades the performance of the maximum torque operation. In the proposed scheme, however, the d-axis current is well regulated to zero and the phase delay in ac current is effectively removed even under such a large variation of L_s.

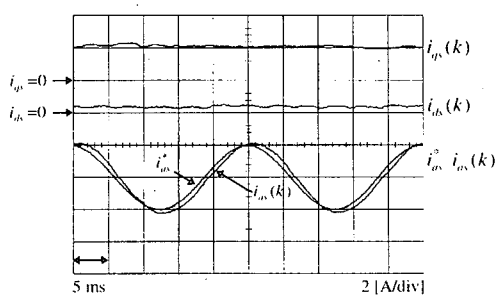

Fig. 7. Conventional predictive current control under $\Delta L_s=0.8L_{so}$

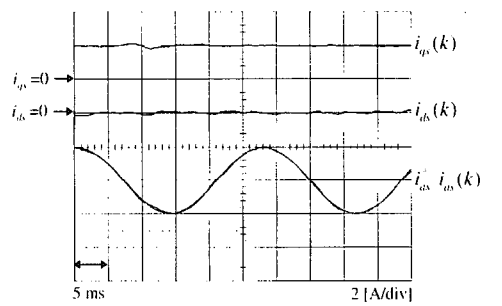

(a) q- and d- axes currents and a-phase current at sampling instant

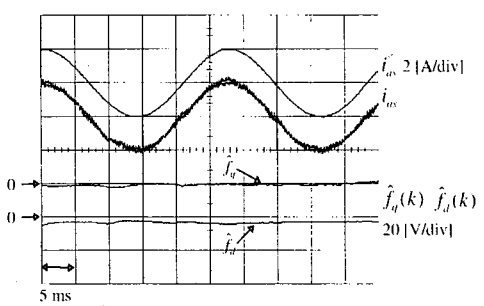

(b) a-phase current and estimated disturbances

Fig. 8. Proposed current control scheme under $\Delta L_s=0.8L_{so}$

Figs. 9 and 10 show the current responses at starting. In the predictive control, the q-axis current error becomes larger since the magnitude of the disturbances is increased as the

rotor speed is increased. However, by the effective disturbance estimation, the q-axis current is well controlled to its reference in the proposed scheme.

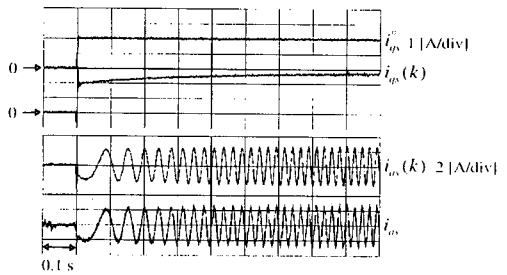

Fig. 9. Conventional predictive current control at starting under $\Delta\lambda_m = -0.5\lambda_{mo}$

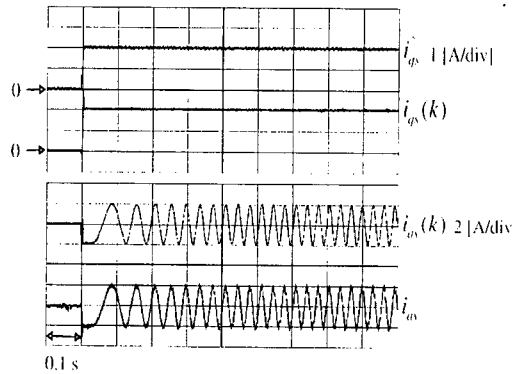

(a) current responses

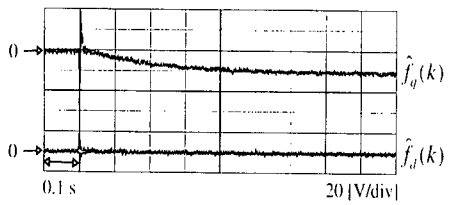

(b) estimated disturbances

Fig. 10. Proposed current control scheme at starting under $\Delta\lambda_m = -0.5\lambda_{mo}$

Figs. 11 and 12 show the control performance when the q-axis current reference is changed from 1 [A] to 2 [A]. In the predictive control, the q-axis current error is shown to be dependent on the operating speed and current level. In the proposed scheme, however, the q-axis current is well controlled to its reference irrespective of the operating speed and current level through the use of an effective disturbance estimation.

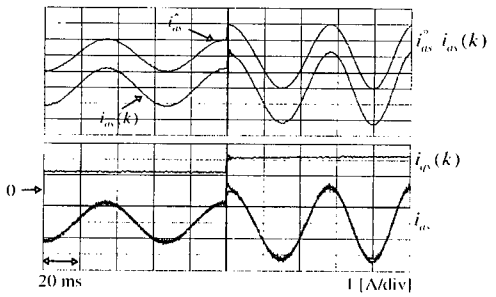

Fig. 11. Control performance of the conventional predictive current control under the step current command change and $\Delta\lambda_m = -0.5\lambda_{mo}$

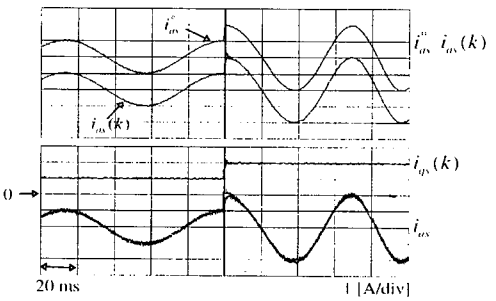

(a) current responses

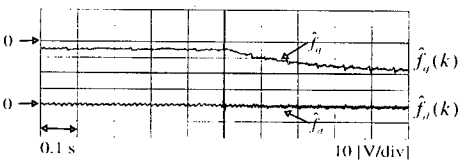

(b) estimated disturbances

Fig. 12. Control performance of the proposed current control scheme under the step current command change and $\Delta\lambda_m = -0.5\lambda_{mo}$

VIII. Conclusions

A simple and robust digital current control technique for a PM synchronous motor under the parameter variations is proposed. Although the predictive control provides an ideal response and a stable performance, its steady-state performance may be degraded under the motor parameter variations or inexact motor modeling. This is more serious at high speed regions. Even though the conventional approaches may deal with this problem, they require a quite complex controller design. To overcome this limitation, the disturbances caused by the parameter variations are estimated

by using a disturbance observer and the estimated disturbances are used for a feedforward control to obtain a robust control performance. Thus, a steady-state current control performance is not affected by the variations of the motor parameters. The whole control system is implemented using the software of DSP TMS320C30 for a PM synchronous motor driven by a three-phase voltage-fed PWM inverter and the effectiveness is verified through the comparative simulations and experiments. As a result, the current control performance can be significantly improved with a relatively simple control algorithm.

References

[1] P. C. Krause, *Analysis of Electric Machinery*. New York: McGraw-Hill, 1986.

[2] T. H. Liu, C. M. Young, and C. H. Liu, Microprocessor-based controller design and simulation for a permanent magnet synchronous motor drive, *IEEE Trans. Ind. Electron.*, vol. IE-35, no. 4, pp. 516-523, Nov. 1988.

[3] D. W. Novotny and R. D. Lorenz, *Introduction to field orientation and high performance AC drives. IEEE* IAS Tutorial Course, 1986.

[4] D. M. Brod and D. W. Novotny, Current control of VSI-PWM inverters, *IEEE Trans. Ind. Appl.*, vol. IA-21, no. 4, pp. 562-570, May/June 1985.

[5] T. M. Rowan and R. J. Kerkman, A new synchronous current regulator and an analysis of current-regulated PWM inverters, *IEEE Trans. Ind. Appl.*, vol. IA-22, no. 4, pp. 678-690, July/Aug. 1986.

[6] H. L. Huy and L. A. Dessaint, An adaptive current control scheme for PWM synchronous motor drives: analysis and simulation, *IEEE Trans. Power Elec.*, vol. 4, no. 4, pp. 486-495, Oct. 1989.

[7] L. Ben-Brahim and A. Kawamura, Digital control of induction motor current with deadbeat response using predictive state observer, *IEEE Trans. Power Elec.*, vol. 7, no. 3, pp. 551-559, July 1992.

[8] D. S. Oh, K. Y. Cho, and M. J. Youn, A discretized current control technique with delayed input voltage feedback for a voltage-fed PWM inverter, *IEEE Trans. Power Elec.*, vol. 7, no. 2, pp. 364-373, April 1992.

[9] K. Y. Cho, J. D. Bae, S. K. Chung, and M. J. Youn, Torque harmonics minimisation in permanent magnet synchronous motor with back EMF estimation, *IEE Proc. Electr. Power Appl.*, vol. 141, no. 6, pp. 323-330, Nov. 1994.

[10] D. C. Lee, S. K. Sul, and M. H. Park, High performance current regulator for a field-oriented controlled induction motor drive, *IEEE Trans. Ind. Appl.*, vol. IA-30, no. 5, pp. 1247-1257, Sep./Oct. 1994.

[11] L. Zhang, R. Norman, and W. Shepherd, Long-range predictive control of current regulated PWM for induction motor drives using the synchronous reference frame, *IEEE Trans. Contr. Syst. Tech.*, vol. 5, no. 1, pp. 119-126, Jan. 1997.

[12] J. S. Meditch and G. H. Hostetter, Observers for systems with unknown and inaccessible inputs, *Int. J. Contr.*, vol. 19, no. 3, pp. 473-480, 1974.

[13] N. Matsui, T. Makino, and H. Satoh, Autocompensation of torque ripple of direct drive motor by torque observer, *IEEE Trans. Ind. Appl.*, vol. IA-29, no. 1, pp. 187-194, Jan./Feb. 1993.

[14] M. Iwasaki and N. Matsui, Robust speed control of IM with torque feedforward control, *IEEE Trans. Ind. Electron.*, vol. IE-40, no. 6, pp. 553-560, Dec. 1993.

[15] J. S. Ko, J. H. Lee, and M. J. Youn, Robust digital position control of brushless DC motor with adaptive load torque observer, *IEE Proc. Electr. Power Appl.*, vol. 141, no. 2, pp. 63-70, Mar. 1994.

[16] K. Ogata, *Discrete-time Control Systems*. Prentice-Hall, 1987.

[17] H. W. van der Broeck, H. C. Skudelny, and G. V. Stanke, Analysis and realization of a pulsewidth modulator based on voltage space vectors, *IEEE Trans. Ind. Appl.*, vol. IA-24, no. 1, pp. 142-150, Jan./Feb. 1988.

[18] T. G. Habetler, F. Profumo, M. Pastorelli, and L. M. Tolbert, Direct torque control of induction machines using space vector modulation, *IEEE Trans. Ind. Appl.*, vol. IA-28, no. 5, pp. 1045-1053, Sep./Oct. 1992.

[19] *TMS320C3x Users Guide*. Texas Instrument, 1990.

[20] *TMS320C30 Assembly Language Tools Users Guide*. Texas Instrument, 1990.

Kyeong-Hwa Kim was born in Seoul, Korea, on March 11, 1969. He received the B.S. degree in Electrical Engineering from Han-Yang University, Seoul, Korea, in 1991, and the M.S. degree in Electrical Engineering from Korea Advanced Institute of Science and Technology(KAIST), Taejon, Korea, in 1993. He is currently working toward th Ph. D. Degree in Electrical Engineering at KAIST. His research interests are in the areas on power electronics and control, which includes ac machine drives and microprocessor-based control applications.

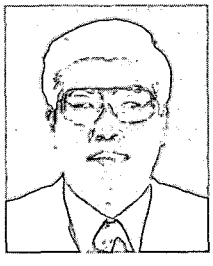

Myung-Joong Youn was born in Seoul, Korea on November 26, 1946. He received the B.S. degree from Seoul National University, Seoul, Korea in 1970 and the M.S. and Ph.D. degrees in electrical engineering from the University of Missouri-Columbia in 1974 and 1978, respectively. He was with the Aircraft Equipment Division of General Electric Company at Erie, Pennsylvania, since 1978, where he was an Individual Contributor on Aerospace Electrical Engineering. He has been with the Korea Advanced Institute of Science and Technology since 1983 where he is now a professor. His research activities are in the areas on power electronics and control which include the drive system, rotating electrical machine design, and high performance switching regulators. Prof. Youn in member of the KIPE, KIEE, AND IEEK.

In-Cheol Baik was born in Seoul, Korea on February 25, 1962. He received the B.S. degree in electronics from Konkuk University in 1984 and the M.S. and Ph.D. degrees in electrical engineering from the Korea Advanced Institute of Science and Technology (KAIST) in 1987 and 1998, respectively. He was a recipient of the University scholarship from Konkuk University during 1980-1982. He has been with the Living system research laboratory of LG Electronics Inc., Seoul from 1987. From February to May 1990, he took the Application Engineer course at SIEMENS Energy & Automation Training Center, Manchester, U.K. His research interests include rotating electrical machine drive systems, electric power conversion systems, and control engineering. Dr. Baik is a member of the Korean Institute of Power Electronics(KIPE) and KIEE.